

Supplementary Materials for

Mitochondrial protein import is regulated by p17/PERMIT to mediate lipid metabolism and cellular stress

Natalia Oleinik, Jisun Kim, Braden M. Roth, Shanmugam Panneer Selvam, Monika Gooz, Roger H. Johnson, John J. Lemasters, Besim Ogretmen*

*Corresponding author. Email: ogretmen@musc.edu

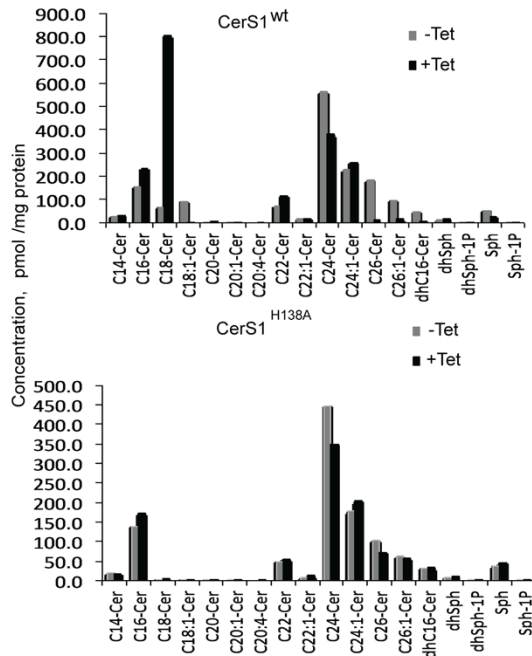
Published 11 September 2019, *Sci. Adv.* **5**, eaax1978 (2019)
DOI: 10.1126/sciadv.aax1978

This PDF file includes:

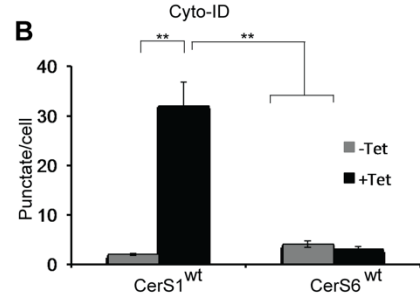
- Fig. S1. Roles of CerS1 versus CerS6 in ceramide generation and mitophagy induction.
- Fig. S2. CerS1 amino acids 60 to 76 are critical for CerS1 import to mitochondria.
- Fig. S3. Ceramide transport by CERT or FAPP2 is not involved in mitophagy.
- Fig. S4. CerS1 mitochondrial import is mediated by p17/PERMIT.
- Fig. S5. Mitochondrial import of CerS1 requires p17/PERMIT and involves amino acids RYE28-30.
- Fig. S6. p17/PERMIT-mediated CerS1 import to mitochondria induces mitophagy.
- Fig. S7. Roles of Drp1 nitrosylation at C644 in mitochondrial localization of CerS1.
- Fig. S8. Mitochondrial localization of CerS1 induces mitophagy via ATG, LC3, and Drp1 in response to SoSe.
- Fig. S9. Mitochondrial CerS1-dependent mitophagy is induced via activation of LC3 and Drp1.
- Fig. S10. Summary of the hypothesis and proposed mechanism for the mitochondrial trafficking of CerS1 by p17/PERMIT.

Figure S1.

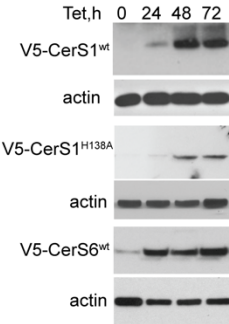
A



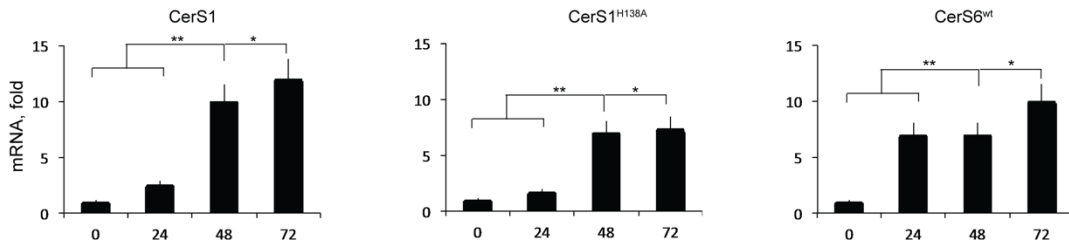
B



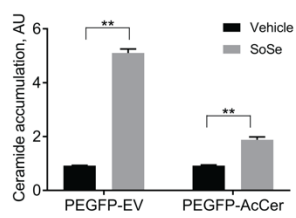
C



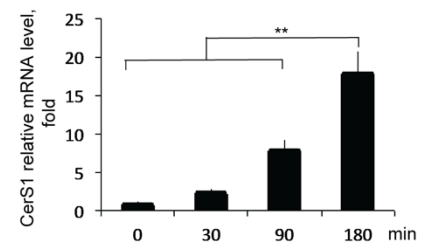
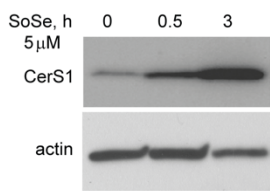
D



E



F



G

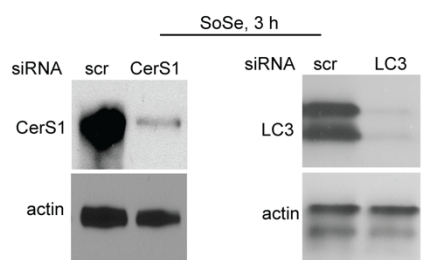
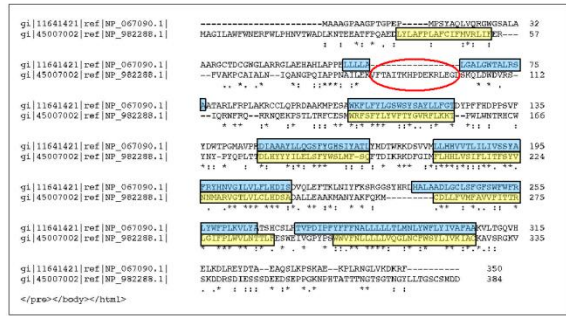


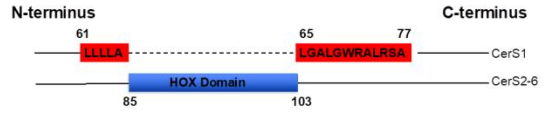
Fig. S1. Roles of CerS1 versus CerS6 in ceramide generation and mitophagy induction. **A**, Ceramide profiles in UM-SCC-22A-Tet-On cells expressing CerS1^{wt} or CerS1^{H138A} mutant upon Dox induction were measured by mass spectrometry-based lipidomics. **B**, Effects of CerS1 vs. CerS6 overexpression on LC3 activation were measured by cyto-ID using flow cytometry in UM-SCC-22A cells (upper panel). MTT assay was performed to measure survival of UM-SCC-22A cells after 72 h Tet-induction of CerS6^{wt}, CerS1^{wt} and CerS1^{H328A} proteins (lower panel). Quantification was performed using at least three independent experiments. **C, D**, Abundance of CerS1^{wt}, inactive mutant CerS1^{H138A} and CerS6^{wt} protein (**C**) and mRNA (**D**) in UM-SCC-22A-CerS1 or UM-SCC-22A-CerS6 cells induced by Dox. Actin was used as a loading control. Data are means \pm SD (n=3 independent experiments, **p < 0.01). **E**, Quantification of ceramide accumulation in UM-SCC-22A cells ectopically expressing acid ceramidase-PEGFP or EV-PEGFP and treated with vehicle or SoSe. Measurements were done by Fiji software using immunofluorescent images with anti-GFP or anti-ceramide antibodies. Data were normalized to GFP-fluorescence. Data are means \pm SD (n=3 independent experiments, **p < 0.01). **F**, CerS1 protein (left panel) and mRNA (right panel) were measured by western blotting and qPCR in UM-SCC-22A cells treated with 5 μ M of Sodium Selenite (SoSe) for 0, 0.5 and 3 h. Actin was used as a loading control. Data are means \pm SD (n=3 independent experiments, **p < 0.01). **G**, CerS1 (left panel) and LC3 (right panel) proteins were measured by western blotting in UM-SCC-22A cells transiently expressing Scr control or CerS1 siRNA (top) or LC3 (bottom) siRNA with/without SoSe. Actin was used as a loading control. Images represent at least three independent experiments.

Figure S2

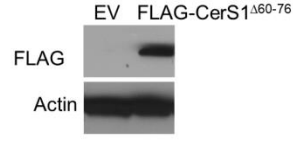
A



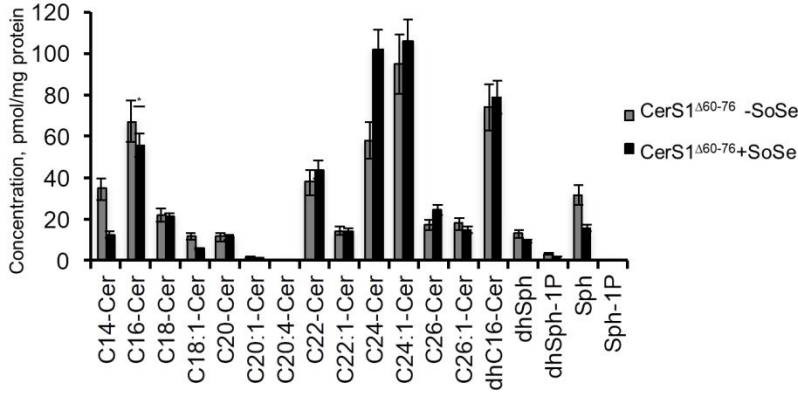
B



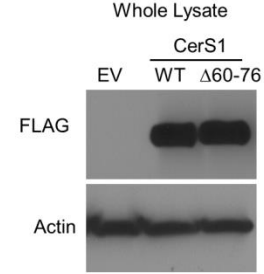
C



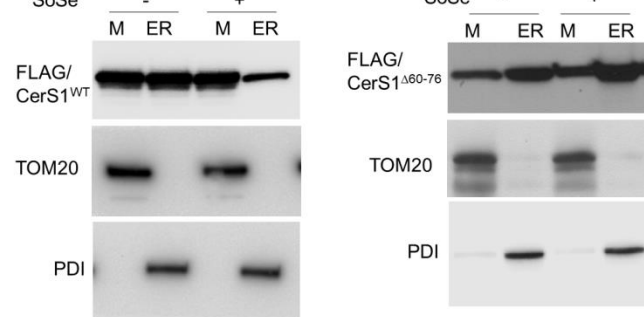
D



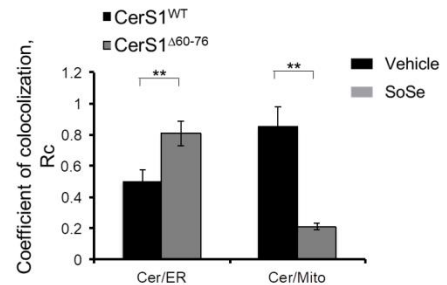
E



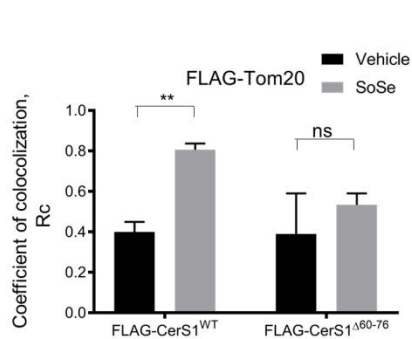
F



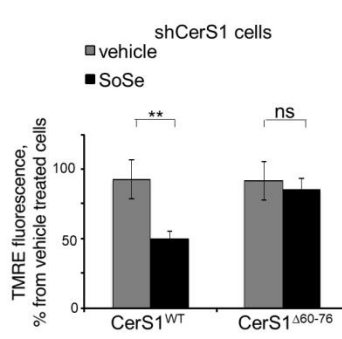
G



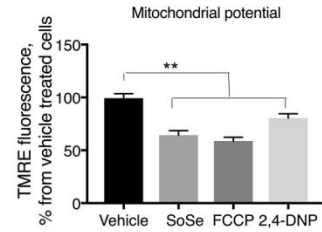
H



I



J



K

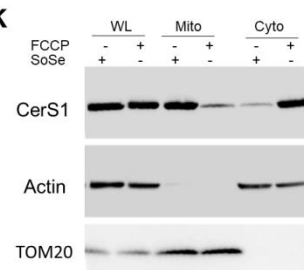
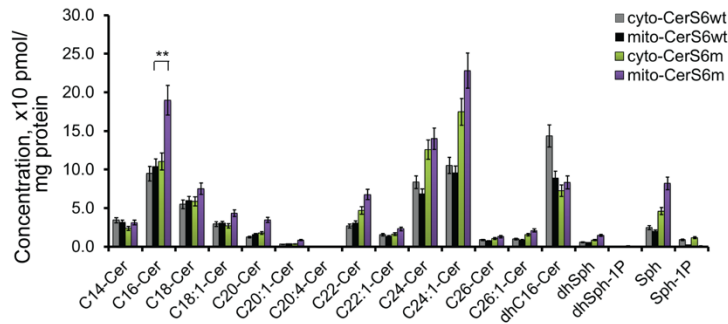


Fig. S2. CerS1 amino acids 60 to 76 are critical for Cers1 import to mitochondria. **A**, Amino acid sequences alignment of human CerS1 and CerS6 proteins. Blue and yellow boxes highlight domains common for all CerS proteins (CerS1-6). Red circle indicates absence of Hox domain in CerS1. **B**, Schematic comparison of CerS1 vs. Cer6 structures. Red box identifies amino acid section unique to CerS1, blue box indicates Hox domain of CerS2-6 proteins. **C**, Abundance of transiently expressed FLAG-tagged CerS1^{Δ60-76} mutant in shCerS1 UM-SCC-22A cells. Images represent three independent experiments. **D**, Ceramide profiles of shCerS1 UM-SCC-22A cells transiently expressing FLAG-tagged CerS1^{Δ60-76} mutant upon exposure to SoSe compared to vehicle-treated control. Data are means ± SD (n=3 independent experiments, *p<0.05). **E**, Cellular lysates of UM-SCC-22A cells transfected with CerS1^{wt} or mutant lacking amino acids 60-76. **F**, Cells treated with SoSe (5 μM, 3 h) were differentially centrifuged and resulting mitochondrial and ER fractions were analyzed using SDS-PAGE. TOM20 and PDI, mitochondrial and smooth ER markers, respectively, were used as loading controls. Images represent at least three independent experiments. **G**, Quantification of confocal images of UM-SCC-22A cells labeled with FLAG and Tom20 after transfection with FLAG-tagged CerS1^{wt} or CerS1^{Δ60-76} and treatment with SoSe. At least three images from three independent experiments were used for quantification. Data are means ± SD (n=3 independent experiments, **p <0.01). **H**, Quantification of confocal images of UM-SCC-22A cells labeled for ceramide and either Tom20, mitochondrial marker, or 11 beta-HSD1, smooth ER marker, upon transfection with CerS1^{wt} or CerS1^{Δ60-76}. Quantification of ceramide and Tom20/11 beta-HSD1 colocalization was performed using Image J software. Data are means ± SD (n=3 independent experiments, **p <0.01). **I**, Mitochondrial potential was measured by TMRE fluorescence in UM-SCC-22A shCerS1 cells transfected with CerS1^{wt} or CerS1^{Δ60-67} treated with/without SoSe compared to

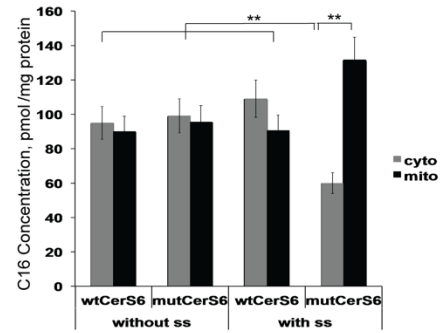
vehicle treated controls with/without SoSe. Data are means \pm SD (n=3 independent experiments, **p <0.01). **J**, UM-SCC-22A cells were treated with SoSe, FCCP or 2,4-DNP, and their effects on mitochondrial membrane potential were measured compared to vehicle-treated controls, upper panel (n=3 independent experiments, **p <0.01). **K**, Effects of SoSe and FCCP on mitochondrial (Mito) versus cytoplasmic (Cyto) localization of CerS1 was measured in UM-SCC-22A cells by Western blotting using anti-CerS1 antibody (lower panel). WL, whole cell lysate. Actin and Tom20 were used as markers for cytoplasmic and mitochondrial markers, respectively. The data shown represent 3 independent studies.

Figure S3.

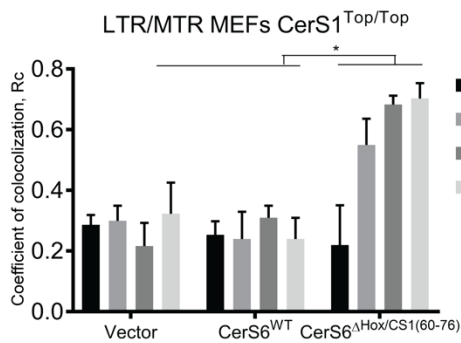
A



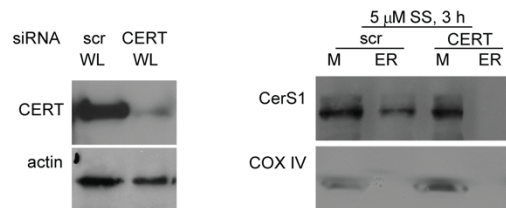
B



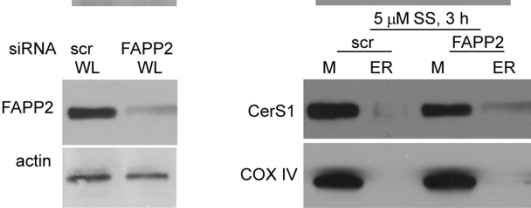
C



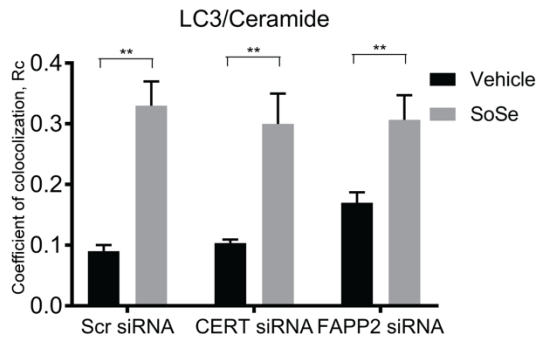
D



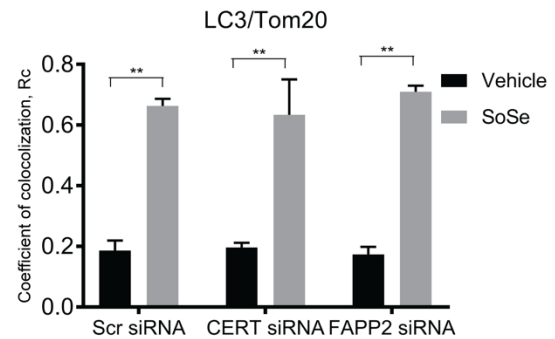
E



F



G



H

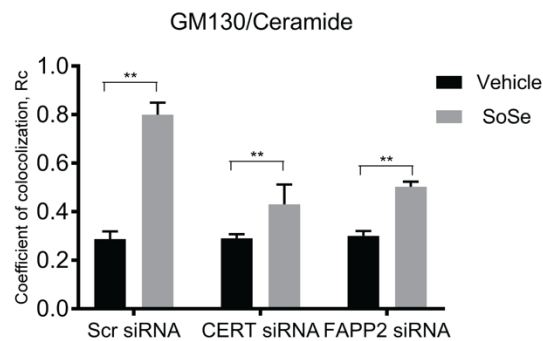


Fig. S3. Ceramide transport by CERT or FAPP2 is not involved in mitophagy. **A**, Total ceramide profiles of mitochondrial and cytosolic fractions of shCerS1 UM-SCC-22A cells transiently expressing FLAG-tagged CerS6^{wt} or CerS6^{ΔHox/CS1(60-76)} (left panel) were measured by lipidomics. **B**, Abundance of C16-ceramide was measured by lipidomics. Data are means ± SD (n=3 independent experiments, **p <0.01). **C**, Quantification of live cell imaging MEFs CerS1^{Top/Top} transiently transfected with vector, CerS6^{wt}, CerS6^{ΔHox/CS1(60-76)}, or CerS1^{wt}, treated with SoSe, and stained with LTG and MTR. Time points were selected to illustrate mitophagy. Images represent at least three independent experiments. Quantification was done using at least three independent experiments. Data are means ± SD (n=3 independent experiments, *p <0.05). **D, E** Localization of CerS1 between mitochondria and ER in UM-SCC-22A cells with transiently silenced CERT (**D**) and FAPP2 using shRNAs (**E**). Successful knockdown of CERT and FAPP2 proteins is confirmed by western blotting. Images represent at least three independent experiments. **F**, Quantification of confocal images showing UM-SCC-22A cells with silenced CERT or FAPP2 upon treatment with SoSe, and stained for ceramide and LC3. Quantification was done using at least three independent experiments. Data are means ± SD (n=3 independent experiments, *p <0.05). **G**, Quantification of confocal images showing UM-SCC-22A cells with silenced CERT or FAPP2 upon treatment with SoSe, and stained for Tom 20 and LC3. Quantification was done using at least three independent experiments. Data are means ± SD (n=3 independent experiments, **p <0.01). **H**, Quantification of confocal images showing UM-SCC-22A cells with silenced CERT or FAPP2 upon treatment with SoSe, and stained for ceramide and GM130. Quantification was done using at least three independent experiments. Data are means ± SD (n=3 independent experiments, **p <0.01).

Figure S4.

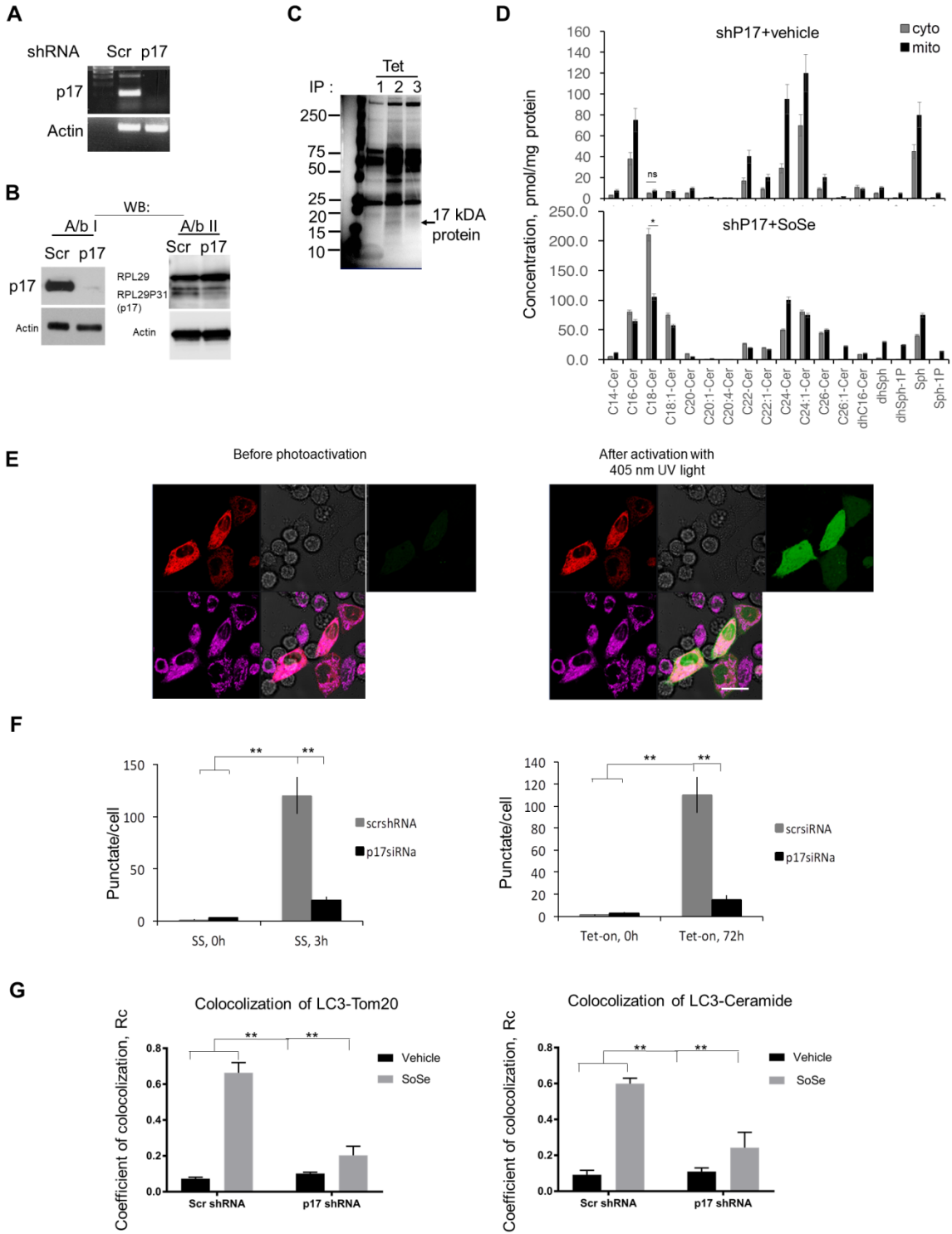


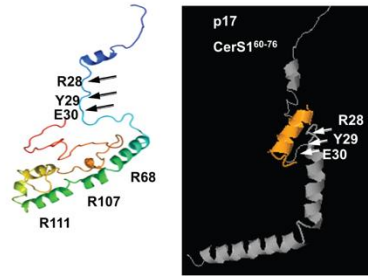
Fig. S4. CerS1 mitochondrial import is mediated by p17/PERMIT. A, B, Levels of p17/PERMIT mRNA (**A**) or protein (**B**) in scrambled and p17 siRNA transfected UM-SCC-22A cells assessed by RT-PCR or western blotting. **C,** Lysates of non-induced and induced for 72 h CerS1-V5 expression UM-SCC-22A Tet-On cells were IP either with IgG or CerS1 antibodies. Proteins were resolved by SDS-PAGE. Coomassie staining of SDS-PAGE demonstrates decrease in abundance of protein corresponding to p17. Images represent at least three independent experiments. **D,** Ceramide profiles of mitochondrial and soluble fractions of P17 siRNA transfected UM-SCC-22A cells upon treatment with vehicle or SoSe were measured by lipidomics. Data are means \pm SD (n=3 independent experiments, *p <0.05). **E,** Photo-activation of PPAGFP-N1-EV (before and after photoactivation) was detected by live cell imaging in HeLa cells (left and right panels). Detection of co-localization of photoactivatable GFP-expressing vector control with ER-RFP or mitotracker (far red) was performed after photoactivation (right panel). **F,** LC3 activation was assessed by Cyto-ID in Scr-siRNA-transfected controls vs. p17 siRNA-transfected UM-SCC-22A cells treated with SoSe (+SoSe, left panel) or Dox (+Tet, right panel). Quantification was performed using Image J. Data are means \pm SD (n=3 independent experiments, **p <0.01). **G,** Quantification of confocal microphotographs of UM-SCC-22A cells treated as in F, and stained for Tom20 and LC3 (left panel), and ceramide and LC3 (right panel). Quantification was done using at least three independent experiments. Data are means \pm SD (n=3 independent experiments, **p <0.01).

Figure S5.

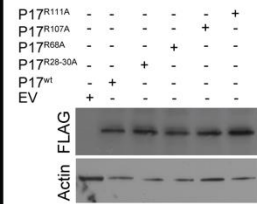
A

>gi|27482992|ref|XP_210334.1| PREDICTED: similar to ribosomal protein L29 [Homo sapiens]
 MAKSKNHSTN NQSRKWRQNG LKKPRKRYE SLKGVDPKFL RNTCFAKKHN
 KVLKMKQAN SAKAVSARAE AIEALVNPKE VKPKIPKGV S RKLDRLAYIA
 HPKLGKRAHA RIVKGLRLCR PKAKAKDQMK AQATAAASVP VRAPRGAQAP
 TKASE

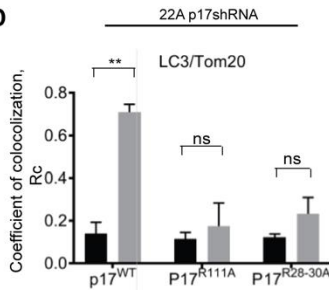
B



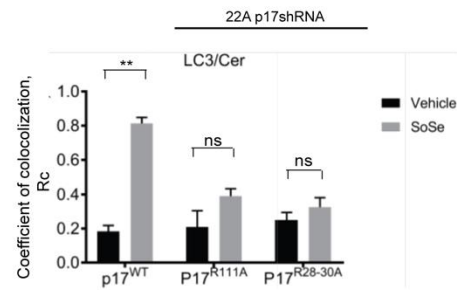
C



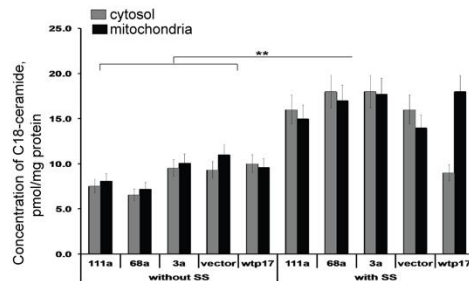
D



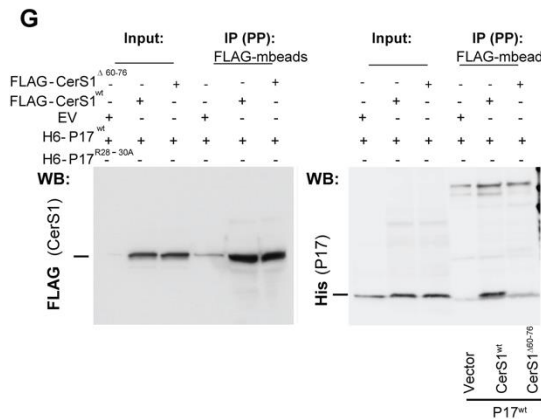
E



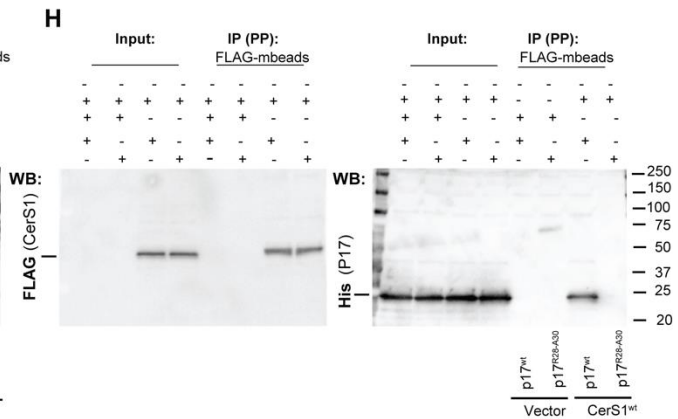
F



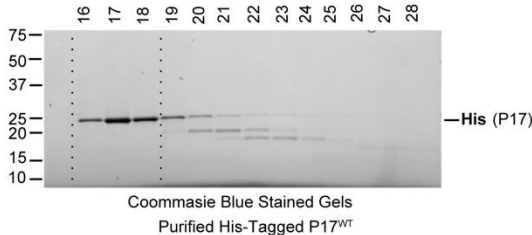
G



H



I



J

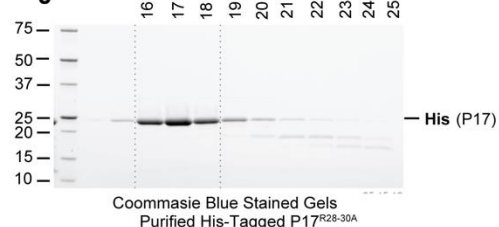


Fig. S5. Mitochondrial import of CerS1 requires p17/PERMIT and involves amino acids RYE28-30. **A**, Amino acid sequence of P17. Highlighted (bold and underscored) residues predicted by SABLE software (<http://sable.cchmc.org>) to be critical for protein binding. **B**, Modeling of p17 (left) predicted by Phyre2 (phyre.com) showing an alpha-helix in N-terminus (blue) domain, and an unorganized C-terminus (orange) domain. Arrows indicate 3 amino acids (Arg28, Tyr29 and Glu30) identified by ZDOCK (predicts protein interaction sites) as most crucial residues for interaction with CerS1 (right). **C**, Abundance of transiently expressed FLAG-tagged p17 (WT and various mutants) in UM-SCC-22A cells expressing shRNA against endogenous p17. Actin was used as a loading control. **D, E**, Quantification of confocal images of SoSe or vehicle treated p17 shRNA-transfected UM-SCC-22A cells transiently expressing vector, p17^{R111A} or p17^{RYE28-30AAA} compared to Scr shRNA-transfected control UM-SCC-22A cells, stained with Tom20 and LC3 (**D**) or ceramide and LC3 (**E**). Quantification was done using at least three independent experiments. Data are means \pm SD (n=3 independent experiments, **p < 0.01). **F**, Abundance of C18-ceramide in p17 or Scr shRNA-transfected UM-SCC-22A cells transiently expressing constructs with various different p17 mutants (R111A, R107A, R68A, RYE28-30AAA) quantified using lipidomics. Data are means \pm SD (n=3 independent experiments, **p < 0.01). **G**, Detection of in vitro association between recombinant purified p17/PERMIT-His (WT) and partially purified CerS1-FLAG (WT and Δ 60-76 mutant with the deletion of residues 60-76) proteins was performed as described in Materials and Methods. CerS1-FLAG expression (WT and mutant) in total lysates (Input), and pulled down CerS1 proteins (WT and mutant) using anti-FLAG antibody conjugated agarose beads were confirmed using anti-FLAG antibody by Western blotting (left panel). Vector-only, empty vector (EV) transfected cell lysates were used as negative controls (left panel). Recombinant WT-

p17/PERMIT-His protein was detected by Western blotting using anti-His antibody (right panel, left three lanes marked as Input). Association between CerS1 (WT and mutant) and p17/PERMIT (WT) was detected in vitro using co-IP and Western blotting using anti-FLAG and anti-His antibodies (right panel marked as IP (PP)). Data represent three independent experiments. **H**, In vitro association between recombinant purified p17/PERMIT-His (WT and R28-30A mutant with RYE-AAA conversion) and partially purified CerS1-FLAG (WT) proteins were performed as described in Materials and Methods. CerS1-FLAG expression (WT) in total lysates (Input), and pulled down CerS1 proteins (WT and mutant) using anti-FLAG antibody conjugated agarose beads were confirmed using anti-FLAG antibody by Western blotting (left panel). Vector-only, empty vector (EV) transfected cell lysates were used as negative controls (left panel). Recombinant WT-p17/PERMIT-His protein was detected by Western blotting using anti-His antibody (right panel, left three lanes marked as Input). Association between CerS1 (WT) and p17/PERMIT (WT and mutant) was detected in vitro using co-IP and Western blotting using anti-FLAG and anti-His antibodies (right panel marked as IP (PP)). Data represent three independent studies. **I**, **J**, Recombinant WT-p17/PERMIT-His (**I**) and R28-30A mutant with RYE-AAA conversion-p17/PERMIT (**J**) were purified as described in Materials and Method, and detected by SDS/PAGE and Coomassie blue staining. Fractions 16-18 were combined to perform in vitro association studies with CerS1.

Figure S6.

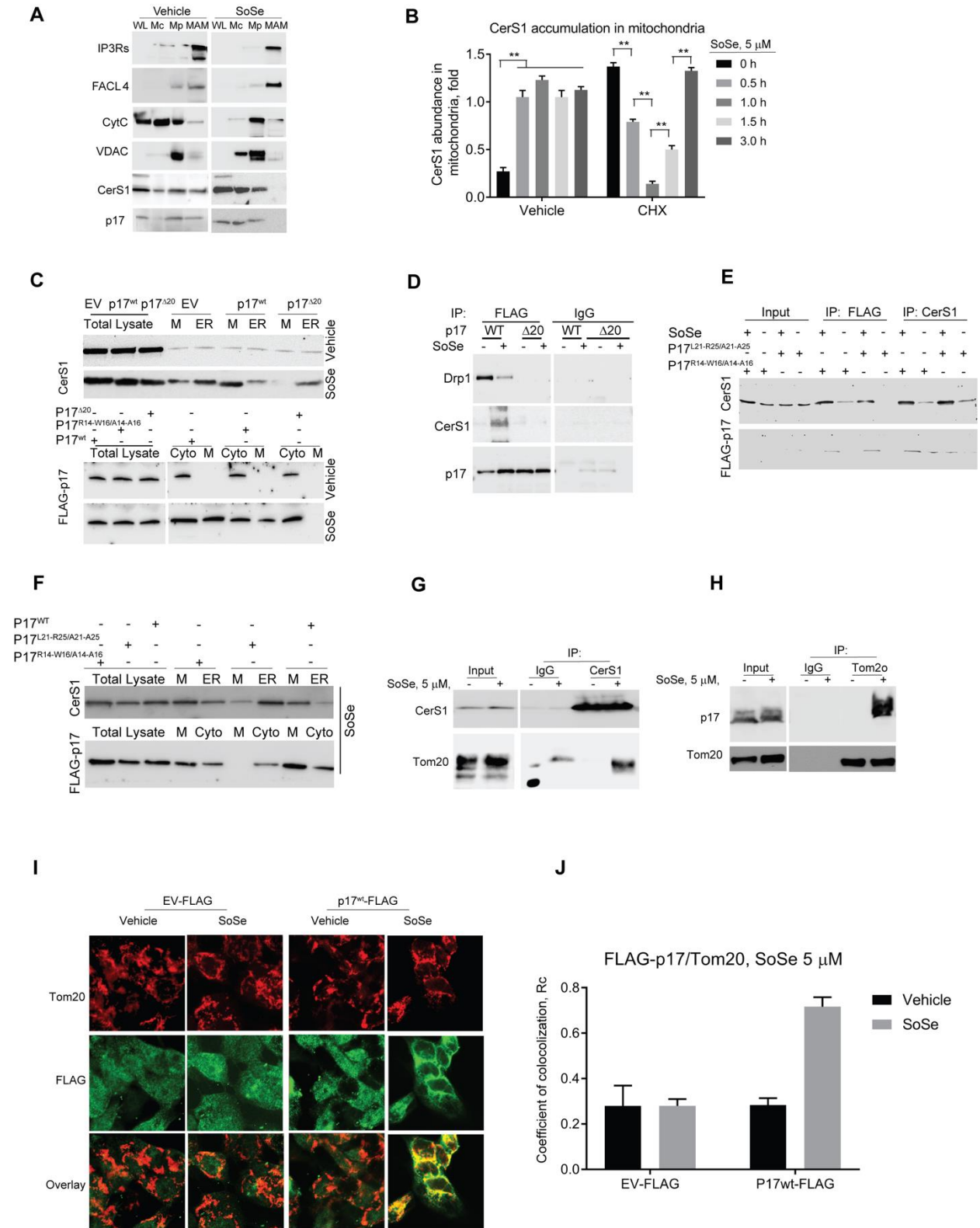


Fig. S6. p17/PERMIT-mediated CerS1 import to mitochondria induces mitophagy. A, Abundance of CerS1 and p17 in whole lysate (WL), crude mitochondria pellet (Mc), pure mitochondria (Mp), and mitochondria associated membranes (MAM) in vehicle (left panel) vs. SoSe-treated (right panel) UM-SCC-22A cells. Purity of fractions was confirmed using subcellular marker proteins: IP3Rs: ER; FAACL4: MAM; Cytochrome C: mitochondria; VDAC: mitochondria and MAM). **B,** Quantification of western blot analysis of newly-synthesized CerS1 protein accumulation in mitochondria of cells pretreated either with vehicle or cycloheximide (CHX; 50 μ g/ml for 3 hours) followed by exposure to SoSe (5 μ M for indicated periods of time). Data is ratio between CerS1 band densities for mitochondrial fraction and for whole lysate. Graph represents means \pm SD (n=3 independent experiments, **p <0.01). **C,** Western blots demonstrate effects of expression of vector-control (EV), p17^{WT}, and p17 ^{Δ 20} on ER and mitochondrial localization of CerS1 in the absence/presence of SoSe. Expression of FLAG-p17 proteins (WT and mutant) was confirmed by western blotting (lower panel). **D,** Association of p17^{WT}, and p17 ^{Δ 20} with Drp1 or CerS1 detected by immunoprecipitation using anti-FLAG antibodies or IgG fraction from non-immune serum as a control followed by western blotting using anti-Drp1, anti-CerS1, or anti-p17 antibodies. **E,** Association of p17/PERMIT^{L21A/R25A} or p17/PERMIT^{R14A/W16A} with CerS1 in the absence/presence of SoSe detected using immunoprecipitation followed by western blotting using anti-FLAG or anti-CerS1 antibodies. **F,** Effects of p17/PERMIT^{WT}, p17/PERMIT^{L21A/R25A} or p17/PERMIT^{R14A/W16A} on ER vs. mitochondrial localization of CerS1 and FLAG-p17/PERMIT detected by western blotting using total cell lysates, or ER, cytosolic, and/or mitochondrial fractions. **G, H,** Interactions between endogenous CerS1 and Tom20 (G), or p17/PERMIT and Tom20 (H) were detected by co-immunoprecipitation and Western blotting using anti-CerS1, anti-p17, anti-Tom20, or anti-IgG

antibodies. Images represent three independent studies. **I, J**, Co-localization of p17/PERMIT^{WT}-FLAG and Tom20 was measured by immunofluorescence in the absence/presence of SoSe. Empty vector (EV)-FLAG-transfected and/or vehicle-treated cells were used as controls (I). Quantification of images were performed by ImageJ. Data are means \pm SD (n=3 independent experiments, **p <0.01)

Figure S7.

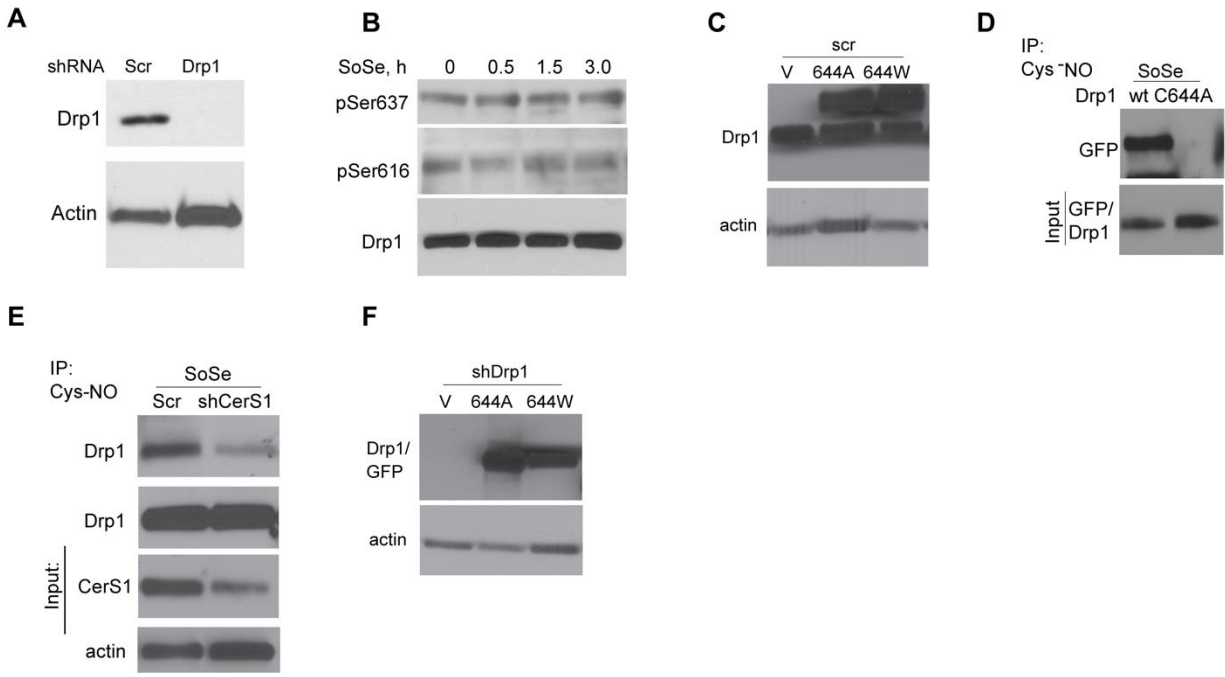


Fig. S7. Roles of Drp1 nitrosylation at C644 in mitochondrial localization of CerS1. A, Levels of Drp1 protein in UM-SCC-22A cells stably transfected with Scr or Drp1 shRNA. **B,** Phosphorylation status of Drp1 at S637 or S616 residues upon exposure to increasing concentrations of SoSe assessed by western blotting using anti-P-Drp1 (S637), anti-P-Drp1 (S616), or anti-Drp1 (total) antibodies. **C,** Precleared lysates of shDrp1 UM-SCC-22A cells transiently expressing GFP-tagged Drp1^{wt} and Drp1^{C644A} mutant and treated with SoSe immunoprecipitated with antibodies to nitrosylated cysteine, resolved on SDS-PAGE and probed with GFP antibodies. Images represent at least three independent experiments. **D,** Precleared lysates of SoSe treated Scr and CerS1 shRNA UM-SCC-22A cells immunoprecipitated with antibodies to nitrosylated cysteine, resolved on SDS-PAGE and probed with Drp1 antibodies. Images represent at least three independent experiments. **E,** Immunoprecipitation of Drp1 and CerS1 using anti-Cys-NO antibody in response to SoSe in UM-SCC-22A cells transfected with Scr-shRNA or CerS1-shRNA. Images represent at least three independent experiments. **F,** Levels of Drp1 in Scr and Drp1 shRNA UM-SCC-22A cells upon expression of empty vector, Drp1^{C644A} and Drp1^{C644W} mutants. Images represent at least three independent experiments.

Figure S8.

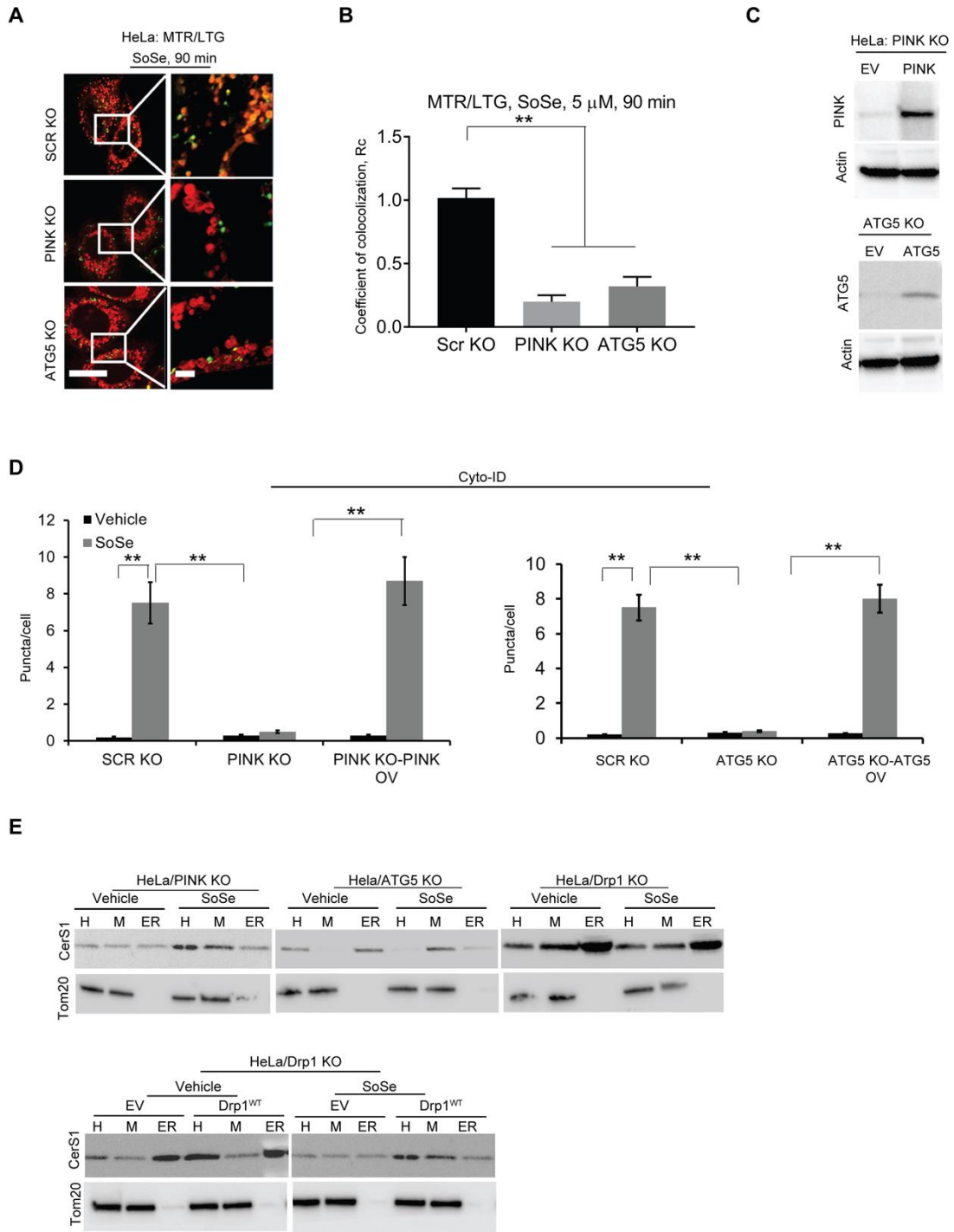


Fig. S8. Mitochondrial localization of CerS1 induces mitophagy via ATG, LC3, and Drp1 in response to SoSe. **A**, Effects of CrispR/Cas9-mediated silencing of PINK1 or ATG5 on mitophagy induction in response to SoSe exposure detected in HeLa cells compared to controls using live cell imaging (left panel). Higher magnification of images are shown (right panel). Images represent three independent studies. **B**, Quantification of live cell imaging of **A**, and co-loaded with MTR (0.5 μ M for 60 min) and LTR (0.5 μ M for 20 min) upon treatment with 5 μ M of SoSe. 90-min time point selected to illustrate onset and completion of mitochondrial digestion by autophagy. Data are means \pm SD (n=3 independent experiments, **p <0.01). **C**, Reconstitution of PINK1 or ATG5 abundance in HeLa cells, in which endogenous PINK1 or ATG5 was silenced using CrispR/Cas9, was confirmed by western blot. Actin used as loading control. Images represent at least three independent experiments. **D**, Effects of ectopic expression of PINK1 or ATG5 on LC3 activation measured using CytoID. These studies represent at least three independent studies. **E**, Effects of ectopic expression of PINK1 or ATG5 on CerS1 mitochondrial trafficking from ER were measured using western blotting (upper panel) in HeLa cells in the absence/presence of SoSe (upper panel). Effects of reconstitution of Drp1 on CerS1 localization in mitochondria in response to SoSe in HeLa cells, with silenced endogenous Drp1 (lower panel). Images represent at least three independent experiments.

Fig. S9. Mitochondrial CerS1-dependent mitophagy is induced via activation of LC3 and

Drp1. **A,** Live cell imaging at 20, 45, 60 and 90 min of HeLa cells in which endogenous Drp1 and LC3 were silenced in the presence of SoSe, and stained with LTG and MTR, shows effects of ectopic expression of vector-only (EV), LC3^{WT}, DRP1^{WT}, and/or DRP1^{C644W} alone or in combination on induction of mitophagy (left panel). Higher magnification of images at 90 min SoSe exposure are shown (**A**, far right column). Quantification of the left panel using ImageJ (upper right panel). Data are means \pm SD (n=3 independent experiments, **p <0.01). **B,** In cells treated with SoSe, autophagic response was evaluated by cytoID. Data are means \pm SD (n=3 independent experiments, **p <0.01). **C,** Ectopic expression of Drp1 and LC3 in HeLa cells, in which endogenous LC3 and Drp1 were silenced, detected by western blotting. **D,** The translocation of LC3-FLAG in whole cell homogenates (H), cytosol (C), or outer mitochondrial membrane (M) with/without SoSe in HeLa cells, in which both Drp1 and LC3 are silenced. Bcl2 was used as marker for outer mitochondrial membrane. **E,** Effects of reconstitution of DRP1 and LC3 on ACO2 degradation due to mitophagy (lanes 1-17) were assessed by western blotting in the absence (upper panel)/presence (lower panel) of SoSe in HeLa cells, in which endogenous Drp1 and LC3 were silenced. The blot shown for the ACO2 detection in response to SoSe (lower panel) contain additional lanes between lanes 15 and 16, which were not part of this study. Those additional lanes were taken out, which were indicated by double lines. Lane 1: CrispR/Cas9 control (2) (Nezich et al, 2015); lane 2: Drp1-knockout (ko)/vector transfection; lane 3: Drp1 ko/Drp1^{WT}; lane 4: Drp1 ko/Drp1^{C644A}; lane 5: Drp1 ko/ Drp1^{C644W}; lane 6: Drp1 k/o/shLC3-vector; lane 7: Drp1 k/o/shLC3-Drp1^{WT}; lane 8: Drp1 k/o/shLC3-Drp1^{C644A}; lane 9: Drp1 k/o/shLC3-Drp1^{C644W}; lane 10: Drp1 k/o/shLC3-LC3^{WT}; lane 11: Drp1 k/o/shLC3-LC3^{F52A}; lane 12: Drp1 k/o/shLC3-Drp1^{WT} + LC3^{WT}; lane 13: Drp1 k/o/shLC3-Drp1^{WT} + LC3^{F52A}; lane 14:

Drp1 k/o/shLC3-Drp1^{C644A} + LC3^{WT}; lane 15: Drp1 k/o/shLC3-Drp1^{C644A} + LC3^{F52A}; lane 16:
Drp1 k/o/shLC3-Drp1^{C644W} + LC3^{WT}; lane 17: Drp1 k/o/shLC3-Drp1^{C644W} + LC3^{F52A}. Data
shown represent three independent studies.

Figure S10

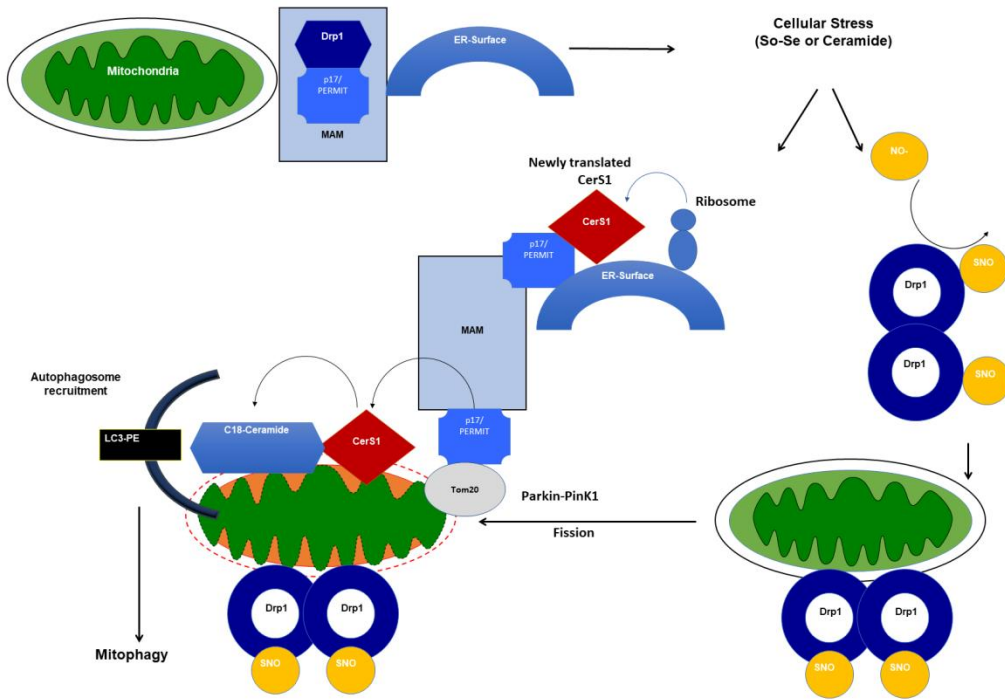


Fig. S10. Summary of the hypothesis and proposed mechanism for the mitochondrial trafficking of CerS1 by p17/PERMIT. In this report, we provide data which suggest that mitochondrial ceramide stress is mediated by trafficking of newly translated CerS1 by a novel protein, p17/PERMIT, from the ER through MAMs. Mechanistically, our data suggest that, in stress-free conditions, Drp1 is associated with p17/PERMIT, forming an inactive complex in the MAMs. Cellular stress, induced either by SoSe or C18-ceramide, mediates Drp1 activation, dependent on the S-nitrosylation of the C644, which then releases p17/PERMIT to retrieve newly translated CerS1 from the ER. Drp1, activated by nitrosylation of C644, then induces mitochondrial fission, resulting in mitochondrial membrane damage. This results in translocation of p17/PERMIT-CerS1 complex to the damaged OMM. Mitochondrial import of CerS1 then results in C18-ceramide generation, inducing recruitment of LC3-II-dependent autophagosomes, involving the F52 of LC3-II, and mediating mitophagy.